

## Design and Simulation of Bioreactor for Crude Oil Bio-desulfurization

Hoda H. Aliga<sup>1,\*</sup>, Asma M. Milad<sup>1</sup>, Miloud Alarabi<sup>2</sup>, Mohamed Aboabboud<sup>3</sup>

<sup>1</sup>Department of Chemical and Petroleum Engineering, Al-Mergib University, Alkhoms, Libya

<sup>2</sup>Department of Chemical Engineering, University of Tripoli, Tripoli, Libya

\*Corresponding Author: hodaelaga2016@yahoo.com

---

### Abstract

Environmental considerations have driven the required to remove sulfur-containing compounds from light oil. The biological removal of sulfur from petroleum feed stocks offers an attractive alternative to conventional thermo-chemical treatment due to the mild operating conditions afforded by the biocatalysts. The aim of this work is to study and simulate the biological desulfurization model and focuses on mass transfer of dibenzothiophene biological transformation. The model used is benzene-water mixture in which oil droplets are the despised phase, the model used to calculate the mass transfer coefficient of benzene in water and the rate of biological desulfurization at temperature range of 20-45 °C, and 10 & 20% of benzene volume fractions. The simulation conducted using a FORTRAN program. The observations found that the time constant was affecting directly with the temperature and sulfur absorption time as well as inversely with the energy capacity. Moreover, the specific surface area is directly proportional to the energy capacity, the volume fraction of benzene in the mixture, sulfur absorption and water purification, but it is changing inversely with increasing the temperature. On the other hand, the energy capacities, the value of the volume fraction of benzene in the mixture and sulfur absorption was influencing on the mass transfer coefficient. The significant results show that the good volume fraction ( $\phi_b$ ) for the best specific surface area is 20%, but the best mass transfer coefficient as well as time constant were obtained at volume fraction 10%. The effect of temperature was slightly low in the proposed medium and on biological desulfurization.

*Keywords:* Bio-desulfurization; Dibenzothiophene; Benzene/water; Crude oil; Simulation.

---

### 1. Introduction

The crude oils contains small amounts of impurities as sulfur compounds that are the most common and harmful impurities in petroleum which decrease its value. The sulfur compounds, ranging typically between 0.05 and 5.0 wt.%, although values as high as 8 wt.% have been reported [1]. These compounds may be an inorganic compounds, mercaptans, aliphatic sulfides, cyclic sulfides or thiophanes disulfides. With no a suitable sulfur-removing step, their use as a fuel results in the formation and emission of polluting sulfur dioxide during combustion [2]. Due to stricter envi-

ronmental legislation, the desulfurization of crude oil and its distillates is becoming increasingly important. A number of conventional methods applied for sulfur removal, which consequently reduce the emission of sulfur compounds to the atmosphere that in turn reduce the environmental pollution. Hydrodesulfurization (HDS) is the most popular chemical method, as well as absorption and biological methods [3]. The biological method as named as bio-desulfurization (BDS) was a concept known for over 50 years [4]. The BDS method uses bacterial strains that are able to remove sulfur from oil, also have a lot of advantages over physical and chemical methods, where,

it does not require high temperature and pressure conditions, but it is usually take long time [5]. Numerous reviews on BDS have been published over the past decade and until the present time [6-12] focusing on fundamental, developing and applied aspect of BDS processes. The efficiency of a bio-desulfurization process basically depends on a sufficient oil/water (o/w) contact, because the reactions proceed mostly at the interface [13, 14]. Bacteria prevail in the water phase, consequently the organic sulfur compounds, e.g. benzo- and dibenzothiophenes must be transferred from the oil bulk phase to the o/w-interface. BDS process operates at ambient temperature and pressure with high selectivity, resulting in decreased energy costs, low emission, and no generation of undesirable side products [15]. The desulfurization rate obtained with crude oil or a petroleum product is an important measurement in determining the suitability of a biocatalyst for an industrial BDS process. Further research into BDS development is required before realistic assessments in pilot-plant studies can be made [16]. Many biological methods used to reduce the sulfur content in crude oil as electro-spray bioreactor, which use of electric field contactors for the bio-desulfurization of the model compound dibenzothiophene (DBT) [17]. Furthermore, in the biochemical conversion process, the bacteria reside in an aqueous phase that mixed with a nonpolar hydrocarbon phase, within this case, the reaction occurs at the aqueous-hydrocarbon interface. During this process, the bacteria attack the sulfur containing aromatic rings and metabolize the sulfur. The removed sulfur ends up in the aqueous phase and can then be separated [17]. The desulfurization of DBT, 4,6 dimethyldibenzothiophene (4,6-DMDBT) and their mixture by lyophilized cells was studied in the presence of dodecane. The desulfurization rate for 4, 6-DMDBT was found to be about 40% in comparison with that for DBT [18]. Stirred tank reactors (STR) are regularly used to generate fine dispersions, since high-energy inputs can be achieved [19]. Furthermore, common relationships describing the dispersion process in a STR are known. In an agitated medium the drop size distribution of the dispersed phase depends on droplet breakage and coalescence [20]. Reactor

operating conditions, physical properties and the volume fraction of dispersed phase, are the factors affecting the average droplet size [21].

In this paper, the mathematical model which conducted by Marcelis et al was used for comparison of the mass transfer rate of DBT within the oil droplet and the biological desulfurization rate. Benzene as a simple hydrocarbon fraction was simulated in the model. The calculations have done by FORTRAN program. The work offered the estimation of the DBT mass transfer rate, expressed by a time constant as a function of the energy capacity ( $W \cdot kg^{-1}$ ) at different o/w-ratios (viz. 10% & 20% (v/v)) and temperatures (viz. 20, 25, 30, 35, 40 and 45°C). The calculated mass transfer rates are compared to reported biological DBT desulfurization rates in order to assess the overall process-limiting step.

## 2. Methodology

### 2.1. Time constant for DBT mass transfer to the benzene/water-interface

For comparison between the mass transfer rate of DBT in the benzene droplet to the benzene/water interface and the biological desulfurization rate, a time constant (b) for the DBT mass transfer in a dispersed phase to the b/w-interface is estimated using an adopted mathematical model [22]. The time constant (or characteristic time) is composed of the reciprocal product of: (i) The mass transfer coefficient ( $K_b$ ) and, (ii) The specific surface area ( $a_{bw}$ ) of the benzene phase and gives an indication of the mass transfer rate. The time constant calculate from the following Equation 2.1 [23]:

$$\tau_b = \frac{1}{k_b * a_{bw}} \quad (2.1)$$

Figure 2.1 shows a schematic representation of the relevant parameters necessary to describe the dispersion process and to estimate  $K_b$  and  $a_{bw}$  in an ideally mixed STR.

The backbone of the dispersion model contains three dimensionless numbers: Reynolds ( $Re$ ), Sherwood ( $Sh$ ) and Weber ( $We$ ). The  $Re$  number expresses the hydrodynamics of the liquid phase, using the input variables density ( $\rho_l$ ), dynamic viscosity ( $\eta_l$ ) and energy capacity ( $\epsilon$ ). The  $Sh$  number gives the characteristics for the mass transfer in the system based on the estimation of the diffusion coefficient ( $D_b$ ) as input variable. The

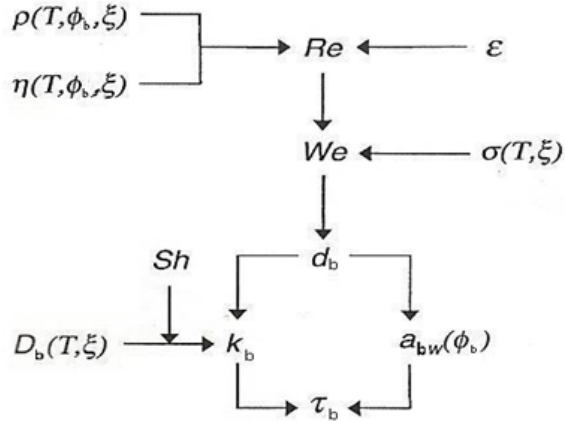


**Figure 2.1:** Chart illustration of the interrelation between the parameters and variables necessary to calculate the DBT mass transfer rate

We number is used to estimate the diameter of the droplets ( $d_b$ ) and depends on the interfacial tension ( $\sigma_{bw}$ ) as input variable. The property input variables  $\rho_l$ ,  $\eta_l$ ,  $D_b$  and  $\sigma_{bw}$  are a function of temperature ( $T$ ), volume fraction of the benzene phase ( $\phi_b$ ) and type of organic phase ( $\xi$ ). To disperse the benzene phase in the aqueous bulk phase energy is required. The energy capacity is defined as the amount of mechanical energy input ( $P$ ) into the system per kilogram reactor content. This variable depends on the liquid density and the vessel geometry and it calculates from Equation 2.2:

$$\varepsilon = \frac{P}{\rho_l * V_l} = N_p * \frac{\rho_l N^3 D^5}{\rho_l \frac{\pi}{4} T_s^2 H} \quad (2.2)$$

Here,  $V_l$  denotes the liquid volume in the STR,  $N_p$  the power number,  $N$  the stirrer speed,  $D$  the impeller diameter,  $T_s$  the tank diameter and  $H$  the liquid height in the tank. The overall density of the total mixed liquid phase ( $\rho_l$ ) depends on the volume fraction of the benzene phase ( $\phi_b$ ) and is a linear combination of the densities of the benzene and water phase. It can be calculated according to Equation 2.3.

$$\rho_l = \phi_b \rho_b + (1 - \phi_b) \rho_w \quad (2.3)$$

To calculate a suitable range of values for  $\varepsilon$  where the mixture is homogeneously dispersed, the following numbers and characteristics were used:  $V_l = 2 \times 10^{-3} \text{ m}^3$ ,  $D = T_s/3.3$ ,  $N_p = 5$  and a range in  $N$  of 8 up to  $25 \text{ s}^{-1}$ . On other hand, Bacteria

thrive in the aqueous phase and it is assumed that the bacteria convert DBT on the interface of the benzene droplets and aqueous phase in the b/w dispersion. The conversion rate is limited by the availability of the b/w surface. The b/w surface can be maximized by minimizing the droplet diameter and by increasing the volume fraction of benzene ( $\phi_b$ ). When the volume fraction of benzene in the b/w dispersion increases, the viscosity of the total mixture will also increase. Therefore, a relation between volume fraction of benzene and dispersion viscosity has to be known. In order to select a maximally acceptable fraction dispersed phase ( $\phi_b$ ) to apply in the model, the following two criteria must be met: (i) the volume fraction of benzene in water exceed 40%. The inversion point is usually uncertain. Therefore,  $\phi_b$  should remain well below 40% in order to be able to describe the behavior of and b/w dispersion accurately. (ii) The dispersion should remain Newtonian; otherwise, a correction for non-Newtonian behavior is necessary. Consequently,  $\phi_b$  may not be higher than 25%. According to these two criteria the maximal value for  $\phi_b$  is 25% [22]. The relative viscosity is defined as the ratio of the dispersion viscosity ( $\eta_{wb}$ ) to that of the continuous aqueous phases ( $\eta_b$ ). The relative viscosity can be calculated using Equation 2.4:

$$\eta_r = \frac{1}{(1 - \phi_b)} \left[ 1 + \frac{1.5 \cdot \eta_r \cdot \phi_b}{\eta_b + \eta_w} \right] \quad (2.4)$$

## 2.2. Calculation of the Average Size of Benzene Droplet

In general, the droplets in the reactor are subject to turbulent conditions, variations in shear forces and pressure. These processes deform the droplets and break them up into smaller droplets, if disruptive forces exceed the interfacial tension forces. The ratio between these forces is expressed in the  $W_e$  number in Equation 2.5.

$$W_e = \frac{C_1 \cdot \rho_w \cdot \varepsilon^{\frac{2}{3}} \cdot d_{max}^{\frac{5}{3}}}{\sigma_{bw}} \quad (2.5)$$

The interfacial tension in the denominator counteracts the disruptive forces in the numerator. After rearrangement, the number in the STR can be defined by Equation 2.6, which can be used for the calculation of maximum attainable droplet diameter.

$$\frac{d_{max}}{D} = C_2 (W_e)_{STR}^{-\frac{3}{5}} \quad (2.6)$$



The droplet diameter is also affected by the volume fraction of benzene ( $\phi_b$ ), since higher coalescence rates occur at higher volume fractions of benzene. Coalescence does not dominate over droplet break-up because  $\phi_b$  is below 25%, therefore the droplet break-up will determine the average size of drop. Due to uncertainties in the drop size distribution, it is not possible to relate the Sauter mean diameter accurately to physical parameters, as is the case for  $d_{max}$ . However, it has been found that  $d_{32}$  is proportional to  $d_{max}$ . Commonly, a linear function of the volume fraction benzene is used to find  $d_{32}$ , as shown by Equation 2.7.

$$\frac{d_{32}}{D} = C_3 (1 + C_4 \phi_b) (We_{STR})^{-\frac{3}{5}} \quad (2.7)$$

Available literature values for the constants  $C_3$  and  $C_4$ , measured under defined experimental conditions, i.e. volume fraction of benzene phase, energy capacity and standard STR geometry, are 0.05 and 13.14 respectively [24]. The mass transfer coefficient can be estimated using the Sherwood number for the dispersed benzene phase, according to Equation 2.8:

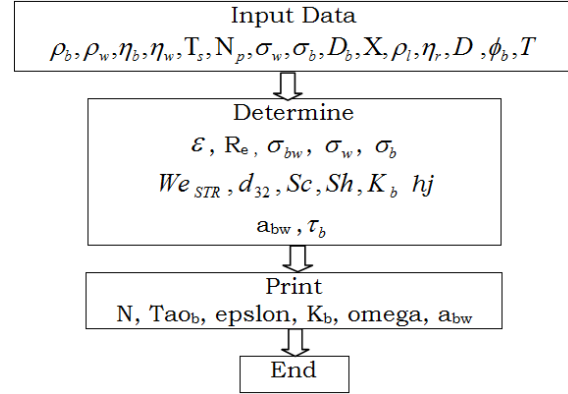
$$K_b = \frac{Sh_b D_b}{X} \quad (2.8)$$

The characteristic length ( $X$ ) of the benzene droplet is assumed to be equal to  $d_{32}$ . The diffusion coefficients ( $D_b$ ) of DBT in the organic phases at various temperatures were estimated using the Wilke–Chang equation [25]. The Sherwood number for rigid and spherical particles was applied. The most relevant characteristics applied as solvent for DBT were summarized in Table 2.1. The specific surface area ( $a_{bw}$ ) is the total surface area of the benzene droplets per cubic meters dispersion and is given by Equation 2.9:

$$a_{bw} = \frac{\sigma \phi_b}{d_{32}} \quad (2.9)$$

### 2.3. Algorithm for Computer Program

The following algorithm illustrated the calculations of this work.



### 3. Results and Discussion

Bio-desulfurization of petroleum is obtained at low temperature and pressure as compared with treatment by hydrodesulfurization under high temperatures and pressures conditions. Bio-desulfurization usually carried out under temperatures (20-45°C) and benzene volume fraction (10% & 20%). This section shows the obtained results which based on a computer program (in Appendix) that contains the mathematical model. The program was used the numerical data of Marcelis et al [22], the obtained results are shown in Figures 3.1,3.2,3.3. In case, volume fraction of benzene in the mixture ( $\phi_b$ ) equal to 0.1, the relationship between the energy capacity and the time constant at 20-45°C temperature was presented in Figure 3.1, where it shows that the decrease in the time constant with the increasing of energy capacity. The relation between the times constant values calculated by the transfer of Dibenzothiophene at variable energy capacity. The values of time constant at  $\phi_{10}$  were the highest, also the time constant was decreased with the increasing of temperatures. The time constant is plotted versus the energy capacity at two  $\phi_{10}$  -values of 10 and 20% (v/v) that especially at = 20% (v/v) low values for the time constant prevail. When comparing between and of the relation between the time constant and energy capacity at variable temperatures, we note the values of time constant at  $\phi_{10}$  are higher for the time constant. In concern of comparison between this study in Figure 3.1 and the study of Marcel's et al. in Table3.1 at T=20°C and  $\phi_b=10\%$ , the decreasing of time constant and the increase of energy capacity were similar to this study [22].

**Table 2.1:** Properties of the applied organic phases at 20 and 45°C

Solvent	Temperature 20 °C			Temperature 45 °C		
	$\rho$ (kg.m <sup>-3</sup> )	$\eta$ ( $\times 10^{-3}$ Pa.s)	$\sigma$ (N.m <sup>-1</sup> )	$\rho$ (kg.m <sup>-3</sup> )	$\eta$ ( $\times 10^{-3}$ Pa.s)	$\sigma$ (N.m <sup>-1</sup> )
Water	997	0.01	72.88E-02	990	0.596	69.18E-02
Benzene	872.9	0.645	0.0350	832	0.386	0.0884

As the time constant is composed of the mass transfer coefficient ( $k_o$ ) and the specific surface area ( $a_{ow}$ ), we investigated the effect of the energy capacity ( $\epsilon$ ) on both parameters. The results are shown in Figure 3.2 and Figure 3.3. The differences in the mass transfer of DBT result from variations in physical properties at different temperature values. This is clearly presented in Figure 3.2 and Table 2.1.

**Table 3.1:** The comparison between energy capacity and the time constant at 20°C

N	Energy capacity (w/kg)	Time (s) (This study)	Time (s) (Mrcelis et al. (2003))
8	1.333	4.827	4.823
9	1.898	3.799	3.795
10	2.604	3.066	3.063
11	3.466	2.526	2.521
12	4.499	2.116	2.111

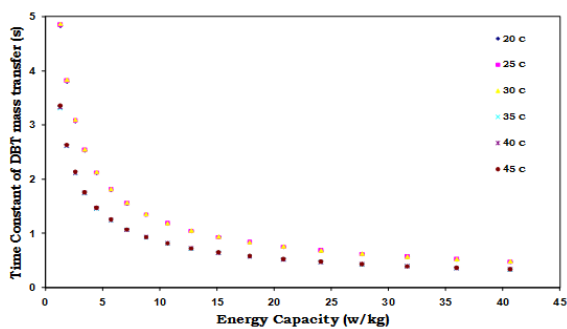


**Figure 3.1:** Time constant of DBT mass transfer vs. energy capacity at 20 to 45°C

However, Figure 3.2 shows that the increase in energy capacity leads to increases the mass transfer coefficient and the increased temperatures decrease the mass transfer coefficient, the optimum value of the mass transfer coefficient was at 20 °C. The variations of the time constants within the fractions were contributed to differences in

the mass transfer coefficients. We note  $\phi_{10}$  give optimum mass transfer coefficient. The effect of the temperature on the mass transfer coefficient clearly manifests for both complex fractions. This effect mainly originates from the influence of temperature on the diffusion coefficient. When comparing between  $\phi_{10}$  and  $\phi_{20}$ , to energy capacity relation with the mass transfer coefficient at temperatures ranging from 20 to 45°C, we note  $\phi_{10}$  give optimum mass transfer coefficient and the highest value is at 20°C.

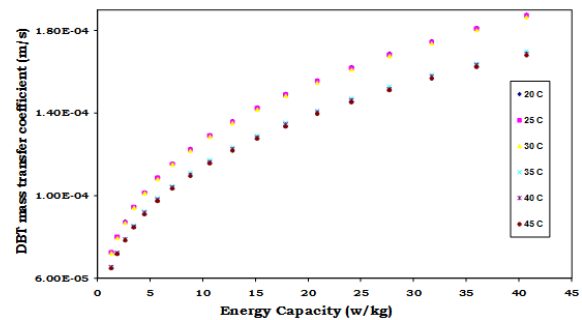


**Figure 3.2:** DBT mass transfer coefficient vs. The energy capacity at temperatures of 20- 45°C

Figure 3.3 shows that the increase in the energy capacity is accompanied the increase of specific surface area. Besides, the optimum specific surface area was estimated at  $\phi_{20}$  and the increased temperatures decrease the specific surface area. The optimum value of specific surface area is recorded at 20 °C. Relatively large time constants are calculated for  $\phi_b$ -values lower than 10% (v/v), as a consequence of the then prevailing low values for the specific surface area. When comparing between , to study the relation between  $\phi_{10}$   $\phi_{20}$  energy capacity and specific surface area at different temperature from 20 to 45 °C, we note the increase in temperatures consequently decrease the specific surface area, the best specific surface area is recorded at  $\phi_{20}$  and 20 °C.

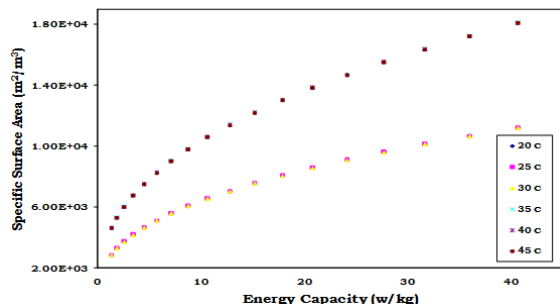


**Figure 3.3:** Specific surface area vs. the energy capacity at temperatures of 20 to 45 °C

#### 4. Conclusion

A mathematical model was adopted in order to study the time constant of DBT mass transfer in a dispersed organic phase in water under a set of conditions using simulations. The model is based on theoretical and semi-empirical equations and it was used to compare the DBT mass transfer in different hydrocarbon fractions in the temperature range of 20–45 °C. The calculated time constants depend mainly on the temperature; dynamic viscosity, the energy capacity, and the hold-up of organic phase (10 or 20%) were found to be in the order of seconds (10-20s). Increasing energy capacity, the difference between the values of the time constants obtained for various simulated conditions becomes negligible (energy capacity has an effect on time constant). The temperature affects the time constant also via the mass transfer coefficient; on the other hand, the temperature dependency of the specific surface area is negligible. The specific surface area depends on the hold-up volume of the organic phase and the interfacial tension. A high specific surface area is favorable for a maximal contact between the bacteria and the benzene phase. Small droplets are not a prerequisite to enhance the DBT mass transfer in the benzene phase, because the diffusion of DBT to the interface is relatively fast.

#### 5. Acknowledgment

The authors gratefully acknowledge the support given for this work by the Al-Mergib and Tripoli University.

#### References

- [1] Grossman J. M.; Lee K. M.; Prince C. R.; Garrett K. K.; George N.G.; and Pickering J. I. Microbial Desulfurization of a Crude Oil Middle-Distillate Fraction: Analysis of the Extent of Sulfur Removal and the Effect of Removal on Remaining Sulfur. *Applied and Environmental Microbiology*, 1999.65, 181-188.
- [2] Babichl, I.V. and Moulijnl J.A. Science and technology of novel processes for deep desulfurization of oil refinery streams. *Fuel*, 2003.82, 607-631.
- [3] Wang, Q.; Hanson J.C.; and Frenkel A.I. Solving the structure of reaction intermediates by time-resolved synchrotron x-ray absorption spectroscopy. *The Journal of Chemical Physics*, 2008.129, 234502.
- [4] ZoBell, C.E. Process for removing sulfur from petroleum hydrocarbons and apparatus. 1953. USA Patent 2,641,564, US Patent Office, <http://www.google.com/patents/US2641564>.
- [5] Ma, C.-Q.; Feng J.-H.; Zeng Y.-Y.; Cai X.-F.; Sun B.-P.; Zhang Z.-B.; Blankespoor H.D.; and Xu P. Methods for the preparation of a biodesulfurization biocatalyst using *Rhodococcus* sp. *Chemosphere*, 2006.65, 165-169
- [6] Grossman, M.J. Microbial removal of organic sulfur from fuels: a review of past and present approaches. In: Ocelli, M.L., Chianelli, R. (Eds.). *Hydrotreating Technology for Pollution Control. Catalysts, Catalysis, and Processes*. Marcel Decker, New York, 1996.345-359.
- [7] McFarland, B.L. Biodesulfurization. *Current Opinion in Biotechnology*, 1999.2, 257-264.
- [8] Ohshiro, T. and Izumi Y. Microbial desulfurization of organic sulfur compounds in petroleum. *Biosci. Biotechnol. Biochem*, 1999.63.
- [9] Monticello, J.D. Biodesulfurization and the upgrading of petroleum distillates. *Current Opinion in Biotechnology*, 2000.540-546.



- [10] Gray, K.A.; Mrachkoyz G.T.; and Squiresy C.H. Biodesulfurization of fossil fuels. *Current Opinion in Biotechnology*, 2003.6, 229-235.
- [11] Srivastava, V.C. An evaluation of desulfurization technologies for sulfur removal from liquid fuels. *RSC Adv.*, 2012.2, 759-783.
- [12] Nuhu, A.A. Bio-catalytic desulfurization of fossil fuels: a mini review. *Rev. Environ. Sci. Bio/Technol.*, 2013.12, 9-23.
- [13] Kaufman, E.N.; Harkins J.B.; and Borole A.P. Comparison of batchstirred and electro-spray reactors for biodesulfurization of dibenzothiophene in crude oil and hydrocarbon feedstocks. *Appl. Biochem. Biotechnol.*, 1998.73, 127-132.
- [14] Shennan, J.L. Microbial attack on sulfur-containing hydrocarbons: implications for the biodesulfurization of oils and coals. *J. Chem. Tech. Biotechnol.*, 1996.67, 109-115.
- [15] Moheballi, G. and Ball A. Biodesulfurization of diesel fuels - Past, present and future perspectives. *International Biodeterioration and Biodegradation*, 2016.119, 163-180.
- [16] Moheballi, G. and Ball A. Biocatalytic desulphurization (BDS) of petrodiesel Fuels". *Microbiology*, 2008.154, 2169-2183.
- [17] Abd El-Latif, F.M., A Study on Sulfur Compounds Removal from Petroleum by Biological Method, in *Chemical 2006*, Alexandria University Alexandria University.
- [18] Mingfang L; Jianmin X; Zhongxuan G; Huizhou L.; and Jiayong C. Microbial Desulphurization of Dibenzothiophene and 4,6 Dimethyldibenzothiophene in Dodecane and Straight-Run Diesel Oil. *Korean J. Chem. Eng.*, 2003.20, 702-704.
- [19] Grossman J.M; Lee K. M; Prince C. R; Minak-Bernero V; G. G.; and Pickering. I. Deep Desulphurization of Extensively Hydrodesulfurized Middle Distillate Oil by *Rhodococcus* sp. Strain ECRD-1. *Applied and Environmental Microbiology*, 2001.67, 1949-1952.
- [20] Harding G.K; Dennis S.J; Blottnitz V.H; and Harrison L.T.S. A life-cycle comparison between inorganic and biological catalysis for the production of biodiesel. *Journal of Cleaner Production*, 2007.16, 1368-1378.
- [21] Hansen M.J.E; Vissenberg J.M; de Beer J.H.V; van Veen R.A.J; and van Santen A.R. Kinetics and Mechanism of Thiophene Hydrodesulphurization over Carbon-Supported Transition Metal Sulfides. *Journal of Catalysis*, 1996.163, 429-435.
- [22] Marcelis, M.L.; Leeuwenb V.M.; Polderman G.H.; Janssen H.J.A.; and Lettinga G. Model description of Dibenzothiophene mass transfer in oil/water dispersions with respect to biodesulfurization. *Biochemical Engineering Journal*, 2003.16, 253-264.
- [23] de-Gooijer, C.D.; Wijffels R.H.; and Tramper J. Growth and substrate consumption of *Nitrobacter agilis* cells immobilized in carrageenan. Part 1. Dynamic modeling, *Biotechnol. Bioeng*, 1991.38, 224.
- [24] Brown, D.E. and K. Pitt. Drop break up in a stirred liquid-liquid contactor. in *Proceedings of the Chemeca*. 1970. Melbourne, Sydney.
- [25] Wilke, C.R. and Chang P. Correlation of diffusion coefficients in dilute solutions. *AIChE J*, 1955.1, 264.

## Appendix

```

Implicit real (a-z)
Integer ::N, T
phaib=0.1
Ts=0.4           !m
Np=5             !constant
H=0.4           !m
Db=1E-10        !m^2/sec
x=0.35          !m
Do 134 T=20, 45, 5
rohW =-0.5726*T+887.94      ! kg/m^3
rohW =-0.3203*T+1005       ! kg/m^3
omegab=-7E-7*T+8E-5       ! kg/m.sec
omegaw=-2E-6*T+0.0001     ! kg/m.sec
segmab=-0.0032*T+0.1028   !N/m
segmaw=-0.0015*T+0.7584   !N/m
rohL=phaib*rohW+(1-phaib)*rohW
omegar=(1/(1-phaib))*(1+(1.5*omegab*phaib)/(omegab+omegaw))
Dt=Ts/3.3
print*, 'T= Celcius',T
    
```



ICCPGE 2016, Al-Mergib University, Alkhoms, Libya

```

print*, '
print*, '
print*, '
Do 233 N=8, 25
Re=rohL*N*(D**2)/omegar
epsilon=Np*((rohL*(N**3)*(D**5))/(rohL*(3.14/4)*(Ts**2)*H))
segmaB=0.035
segmaW=0.72
segmaT=segmaB+segmaW
westr=(0.4*rohW*(epsilon**0.667)*(0.08**1.667))/segmaT
d32=D*0.051*(1+3.14*phaib)*(westr**(-0.6))
sc=N/Db
sh=2+0.6*(Re**0.5)*(sc**0.3333)
Kb=(sh*Db/x)*10
abW=(6*phaib/d32)*10
Taob=1/(Kb*abW)
print*, N, Taob, epsilon, Kb, omegar, abW
233 Enddo
134 Enddo
stop
end

```